—報告—
Report

Improvement of shipborne sky radiometer and its demonstration aboard the Antarctic research vessel *Shirase*

Noriaki Tanaka[1*], Hiroshi Kobayashi[2], Toshiyuki Murayama[3] and Masataka Shiobara[4, 5]

船舶用スカイラジオメータの改良および南極観測船「しらせ」での初期観測結果

田中典章[1*]・小林　拓[2]・村山利幸[3]・塩原匡貴[4, 5]

(Received February 14, 2014; Accepted June 16, 2014)

要旨: 動揺する船上においても太陽直達光を観測できるように，船舶用スカイラジオメータの太陽追尾性能を改良した．改良点は，太陽追尾精度の向上，測器視野角の拡大，太陽追尾速度の迅速化および測定手法の改良である．改良後の装置を用いて，第 51 次および第 52 次日本南極地域観測隊の本観測時に，南極観測船「しらせ」船上において太陽直達光および天空輝度分布を測定し，動揺した船上での直達光観測に成功した．直達光から算出された波長 500 nm における大気エアロゾルの光学的厚さは 0.01–0.34 であり，東南アジアおよび春季の西太平洋上で高い値を示した．オングストローム指数は－0.06～2.00 の範囲であり，東南アジアおよびシドニー付近で最大を示した．今後，船舶用スカイラジオメータが，海洋上の大気エアロゾルに関する知見を深めると期待される．

Abstract: The sun-tracking performance of a shipborne sky radiometer was improved to attain accurate aerosol optical thickness (AOT) from direct solar measurements on a pitching and rolling vessel. Improvements were made in the accuracy of sun-pointing measurements, field-of-view expansion, sun-tracking speed, and measurement method. Radiometric measurements of direct solar and sky brightness distribution were performed using the shipborne sky radiometer onboard the Antarctic research vessel (R/V) *Shirase* during JARE-51 (2009–2010) and JARE-52 (2010–2011). The temporal variation of signal intensity measured by the radiometer under cloudless conditions was smooth, demonstrating that the radiometer could measure direct sunlight onboard the R/V. AOT at 500 nm ranged from 0.01 to 0.34, and values over Southeast Asia and over the western Pacific

[1] 山梨大学大学院医学工学総合教育部．Interdisciplinary Graduate School of Medicine and Engineering, University of Yamanashi, 4–3–11 Takeda, Kofu, 400-8511.
[2] 山梨大学大学院医学工学総合研究部．Interdisciplinary Graduate School of Medicine and Engineering, University of Yamanashi, 4–4–37 Takeda, Kofu, 400-8510.
[3] 東京海洋大学海洋科学技術研究科．Graduate School of Marine Science and Technology, Tokyo University of Marine Science and Technology, 2–1–6 Etchujima, Koto-ku, Tokyo 135-8533.
[4] 情報・システム研究機構国立極地研究所．National Institute of Polar Research, Research Organization of Information and Systems, Midori-cho 10–3, Tachikawa, Tokyo 190-8518.
[5] 総合研究大学院大学複合科学研究科極域科学専攻．Department of Polar Science, School of Multidisciplinary Sciences, SOKENDAI (The Graduate University for Advanced Studies), Midori-cho 10–3, Tachikawa, Tokyo 190-8518.
* Corresponding author. E-mail: g14de002@yamanashi.ac.jp

南極資料，Vol. 58，No. 3，341–351，2014
Nankyoku Shiryô (Antarctic Record), Vol. 58, No. 3, 341–351, 2014

Ocean in spring were higher than those over other regions. The Ångström exponent ranged from −0.06 to 2.00, and values over Southeast Asia and off the coast near Sydney were the highest. The improved shipborne sky radiometer will contribute to a good understanding of the nature of aerosols over the ocean.

1. Introduction

Atmospheric aerosols affect the earth's climatic system through the scattering and absorption of solar radiation (direct effect) and modification of cloud properties (indirect effect) (IPCC, 2007). An understanding of the global spatial and temporal variations of aerosol optical properties, including aerosol optical thickness (AOT), is necessary for accurate assessment of the global radiation budget (Kaufman *et al.*, 1997). The Aerosol Robotic Network (AERONET) initiated by NASA (Holben *et al.*, 1998) and the Sky Radiometer Network (SKYNET; http://atmos.cr.chiba-u.ac.jp/; Takamura *et al.*, 2004), located mainly in eastern Asia, are worldwide networks of ground-based sites for monitoring aerosol optical properties. Data from these networks function as validation sources of satellite retrievals of aerosol optical properties.

Oceans cover approximately 70 % of the earth's surface and produce a large quantity of natural aerosols that affect the earth's climatic system. Sea salt is a major component of maritime aerosols. Aerosols over the ocean, however, contain a dust, particles from biomass burning, and other anthropogenic aerosols (Andreae, 2007). Thus, investigation of aerosol optical properties over the ocean is important for the estimation of the global radiation budget. Recently, AOT over the ocean has been measured using a handheld sun photometer as part of the Maritime Aerosol Network, which was developed as a component of AERONET (Smirnov *et al.*, 2009) and the NASA program Sensor Intercomparison and Merger for Biological and Interdisciplinary Oceanic Studies (SIMBIOS; Knobelspiesse *et al.*, 2004). However, these observation networks have very limited coverage of vast oceanic areas (Smirnov *et al.*, 2009).

An earlier shipborne sky radiometer that automatically measured the direct sun radiation and sky radiance distribution was improved to raise the quality and quantity of aerosol optical property data over the ocean. The sun-tracking system of this earlier sky radiometer was prone to fail in tracking the sun because of the rolling and pitching of the vessel. This was due to the instrument's low axial resolution, narrow error tolerance for sun pointing, and low sun-tracking speed. Therefore, the sun-tracking performance of the radiometer was improved to obtain higher accuracy of AOTs from direct sun measurement, even under conditions of substantial rolling and pitching of the vessel. This improved radiometer was called the POM-01 Mk3 (Prede Co., Ltd., Tokyo, Japan). In this study, measurements were taken onboard the Antarctic research vessel (R/V) *Shirase* during the 51st Japanese Antarctic Research Expedition (JARE-51; 2009–2010) and JARE-52 (2010–2011) to assess the sun-tracking performance of POM-01 MK3. As part of the JARE activities, the R/V *Shirase* navigates a regular track every year between Tokyo, Japan and Syowa station, Antarctica, during November–December (going to Antarctica by way of Fremantle, Australia) and February–April (returning from Antarctica by way of Sydney, Australia). Observations onboard the R/V along this course can be used to measure the optical properties of

various atmospheric aerosol particles (Yabuki *et al.*, 2003).

Here, we initially describe the improvements of the shipborne sky radiometer. Then, we discuss the AOT and Ångström exponent (AE) calculated using direct solar data measured by POM-01 MK3 during JARE-51 and JARE-52.

2. Method

2.1. Instrument

A ground-based sky radiometer is an instrument that measures both direct solar radiation and the distribution of sky radiance (e.g., Aoki and Fujiyoshi, 2003; Shiobara *et al.*, 1991). These radiometers typically comprise a sun- and sky-scanning spectral radiometer with 1° full-angle field-of-view, sun sensor, scanning device, and control unit. The sun sensor points directly at the sun, and the sky radiance distribution is measured automatically by the spectral radiometer scanning azimuth angle ϕ at almucantar and solar zenith angle θ. In the monitoring of aerosol optical properties, only data unaffected by cloud in the direction of the sun are used.

The earlier version of the shipborne sky radiometer was developed to measure the direct solar and sky radiance distribution from a moving vessel, and it was manufactured based on a ground-based sky radiometer with the following additions. A narrow field-of-view charge-coupled device (CCD) camera was attached to the bottom of the sun sensor to expand the range of sun detection, a wide field-of-view CCD camera was fixed atop the sun tracker to record the sun's position to obtain the solar azimuth, and a GPS receiver and a barometer were attached to the sky radiometer. However, the sun-tracking system of the earlier version had difficulties functioning on a rolling and pitching vessel. Therefore, four modifications were made to the sun-tracking performance to obtain high-accuracy AOTs from the direct solar measurements, despite the considerable rolling and pitching of the vessel. The first modification was to improve the accuracy of the sun-pointing measurements. The narrow field-of-view CCD camera was replaced by a position-sensitive detector with higher axial resolution. The second improvement was the expansion of the field-of-view. The full-angle field-of-view of the radiometer was expanded from 1° to 1.5°, which increased the sun pointing error tolerance. The third improvement was in the sun-tracking speed. Stepping motors in the sun-tracking system were replaced by DC servomotors with high-speed response. The final enhancement was made to the measurement method. Signal intensities at each wavelength (380, 400, 500, 675, 870, 940, and 1020 nm) were maximum values, repeated three times for each wavelength. This was done to remove errors in the direct solar measurement caused by sun-pointing errors of the sky radiometer.

We made direct solar and sky radiance measurements using POM-01 MK3 as part of JARE-51 and JARE-52. Figure 1 shows the cruise tracks of the R/V *Shirase* in JARE-51 (left) and JARE-52 (right). A broken line indicates a track during which the instrument failed. Direct solar measurements were made every 2 min and sky radiance measurements every 10 min. Generally, the AOT at the wavelength of 500 nm is used for discussing aerosol loading because the 500-nm wavelength is the strongest solar radiation wavelength, and has the highest signal-to-noise ratio of the measurement. Thus, we mainly discuss the AOT at the 500-nm wavelength in this paper. Data from other wavelengths (380, 400, 500, 675,

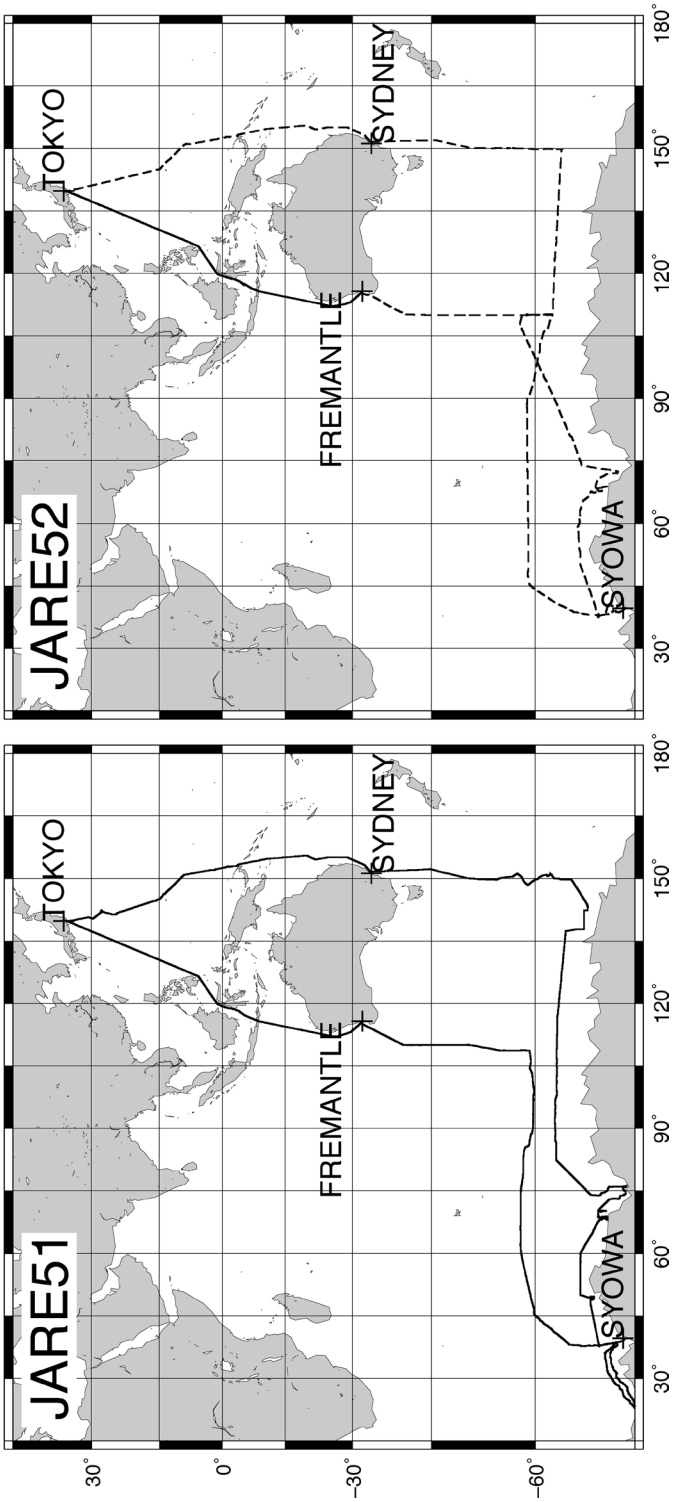

Fig. 1. Cruise tracks of the R/V Shirase during JARE-51 (left) and JARE-52 (right). The broken line indicates portions of the track where the instrument failed.

870, and 1020 nm) are discussed with regard to the AE calculation. The 940-nm wavelength is the water vapor channel, which is excluded from the discussion in this paper.

For the sky radiance measurements, the direction of the sun detected by the wide field-of-view CCD camera is defined as 0° azimuth. The sky radiance distribution is measured automatically by the spectral radiometer scanning azimuth angle ϕ at almucantar and solar zenith angle θ. However, we were unable to obtain good results for sky radiance distribution. There was a large gap between the actual and recorded scattering angles in the measurements because of the low speed of image processing by the CCD camera. Therefore, POM-01 MK3 has room for further improvement.

2.2. Analyses

AOT was calculated only from direct solar intensity. From the Beer–Bouguer–Lambert law, direct solar intensity is given by

$$F(\lambda) = F_0(\lambda) \exp(-m_0 \tau(\lambda)), \tag{1}$$

where F_0 is the flux at the top of the atmosphere, m_0 the optical air mass, and τ the optical thickness at wavelength λ, which is the sum of the aerosol, Rayleigh, and ozone optical thicknesses. AOT is obtained by subtraction of the Rayleigh and ozone optical thicknesses from τ. The calculations of AOT, Rayleigh, and ozone optical thicknesses were based on the SKYRAD algorithm version 4.2 (Nakajima *et al.*, 1996). Rayleigh optical thickness was calculated based on the atmospheric pressure from the barometer built into the sky radiometer and ozone optical thickness was determined from the value of total ozone. That value was interpolated linearly from the mean of 3 days obtained by the Ozone Monitoring Instrument (http://ozoneaq.gsfc.nasa.gov/) at each measurement point.

The AE is defined as α in the following:

$$\tau_A(\lambda) = \beta \lambda^{-\alpha}, \tag{2}$$

where τ_A is the AOT at each wavelength λ and β the turbidity coefficient. The AE is obtained by the method of least squares from the derived AOTs at each wavelength. The value of AE is used as an indicator of the size distribution. Higher values of AE mean that the relative amount of small particles in the size distribution is high.

The following procedure was applied to remove data that were influenced by the attenuation of solar radiation intensity due to cloud, exhaust gas contamination, and pointing errors. (1) Measurements were grouped into 10-min series. Any data series in which the portion of standard deviations of any AOT at each wavelength exceeded 5 % was removed. (2) Smirnov *et al.* (2009) indicated that for AE greater than -0.1, a point in sun photometer measurements is considered cloud and pointing error-free. Therefore, for AE equal to or less than -0.1, data were considered to have cloud and pointing errors and were removed. (3) The R/V *Shirase*'s smokestacks were located behind the instrument. Therefore, data with a relative wind direction between 120° and 200° clockwise from the bow direction, and with a solar azimuth angle between 120° and 200° in that direction, were removed as potentially exhaust-gas contaminated. (4) Finally, we determined whether the data had cloud- or exhaust-gas contamination or pointing errors by visually checking the variability of direct solar intensity and cloud amount during daytime.

Shipboard meteorological data including wind direction and speed were recorded every 5 s onboard the R/V. Data of each meteorological parameter were interpolated linearly to coincide with the time of the sky radiometer measurements.

3. Results and discussion

3.1. Sun-tracking experiment using the shipborne sky radiometer

We performed a sun-tracking experiment to simulate actual conditions. Direct solar measurements were made using POM-01 MK3 mounted on a test bench that rolled/pitched with 5° amplitude and a 10-s cycle. Figure 2 shows a portion of the results of the sun-tracking experiment from June 10, 2008. This figure shows that the measured direct solar intensities were stable in a rolling and pitching environment, demonstrating the radiometer's ability to perform the measurements and continue direct tracking of the sun under such conditions.

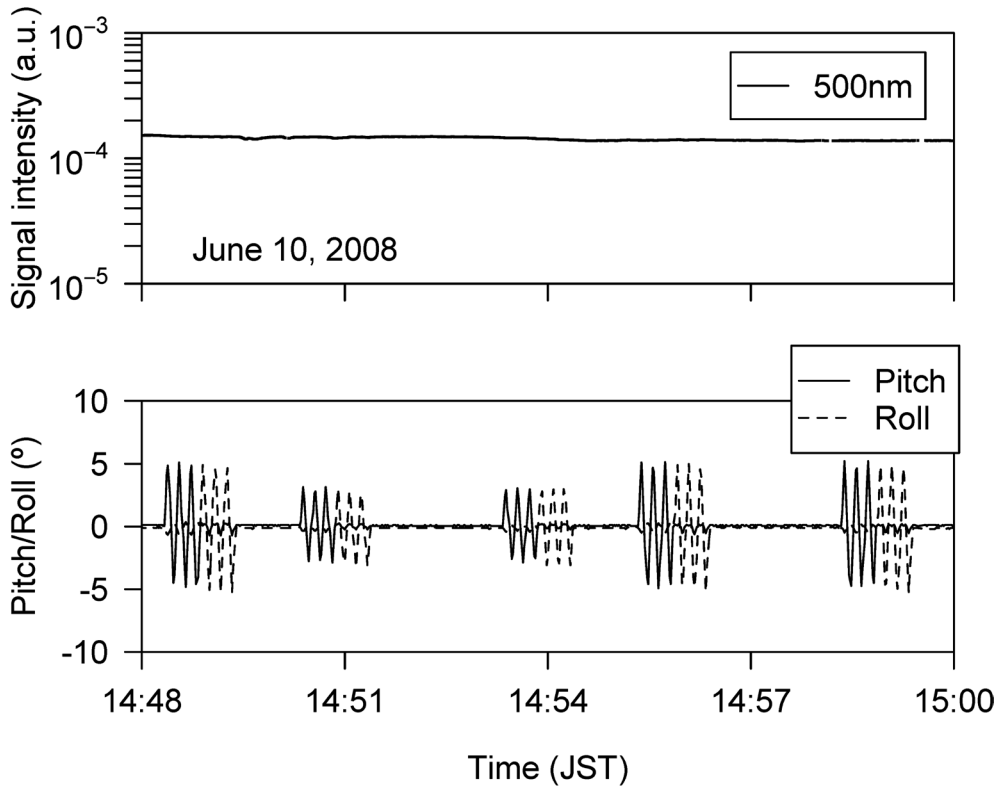

Fig. 2. Time series of direct solar intensity (upper), and pitching and rolling (lower) during the sun-tracking experiment. Time is represented as Japan Standard Time (JST; Universal Time + 9 h).

3.2. Measurement results in JARE-51 and JARE-52

The upper panel of Figure 3 shows a time series of direct solar intensity at 500 nm on March 24, 2010 under clear skies. The pitch angle of the vessel ranged from −2.2° to 2.8° and the roll angle ranged from −3.4° to −0.3° during the time of observation. Most of the variation in the data is smooth, but there are distinct decreases in signal intensity due to the radiometer pointing at vessel structures, including the mast. The middle panel of the figure shows the AOT at 500 nm and the lower panel shows screened results. In instances of sharply higher AOT values, data were removed around the error values.

Solar calibration constants of the sky radiometer were determined by field observation using the Langley-plot method (Shaw *et al.*, 1973). This method retrieves F_0 from a plot of

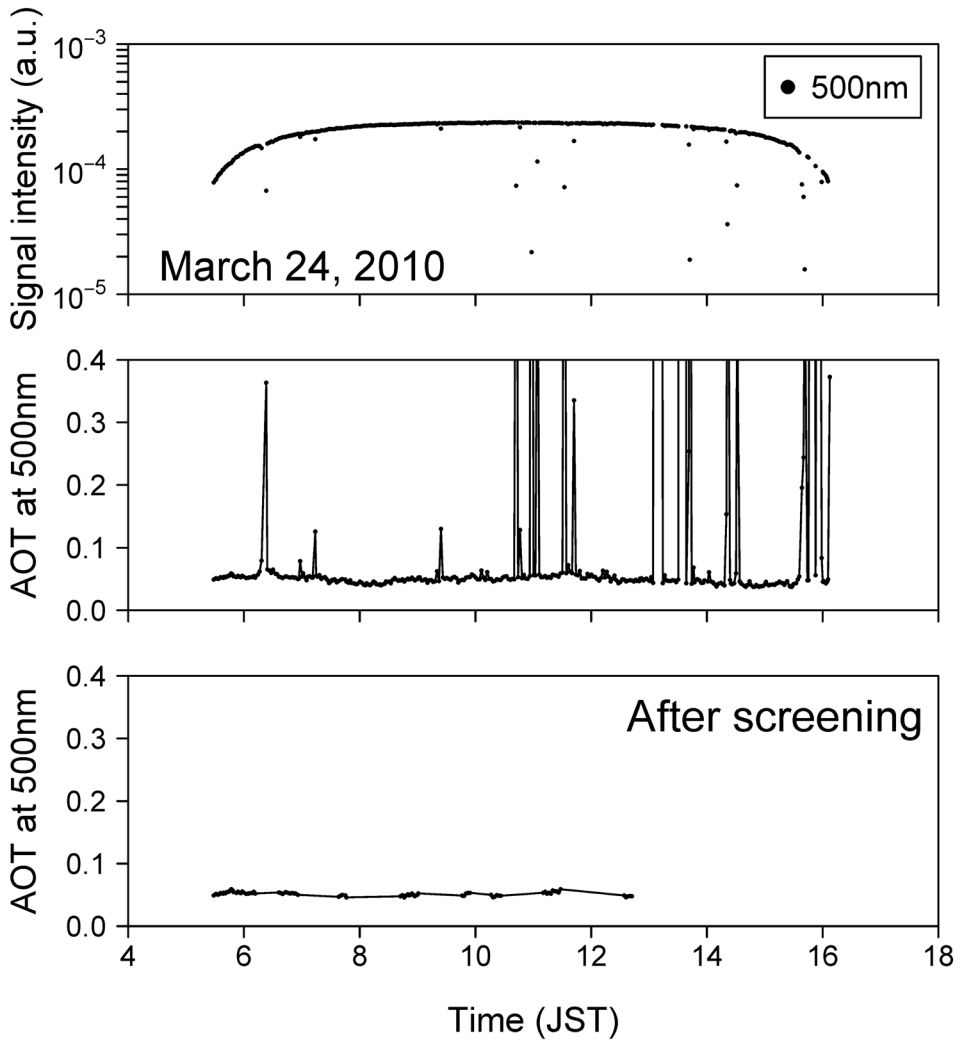

Fig. 3. Time series of measured direct solar intensity at wavelength 500 nm on March 24, 2010 (upper), aerosol optical thickness (AOT) at the same wavelength (middle), and screened results (lower).

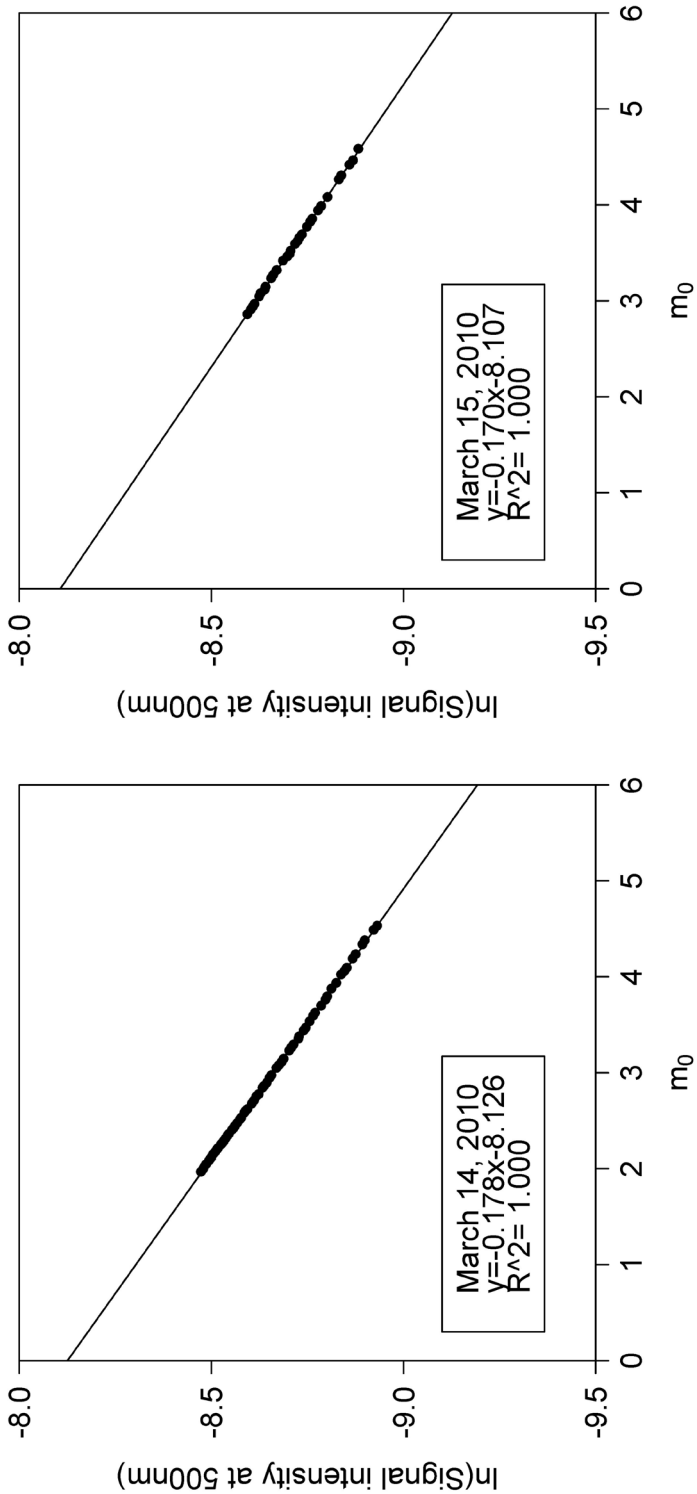

Fig. 4. Langley plots at a wavelength of 500 nm measured on March 14, 2010 (left) and March 15, 2010 (right).

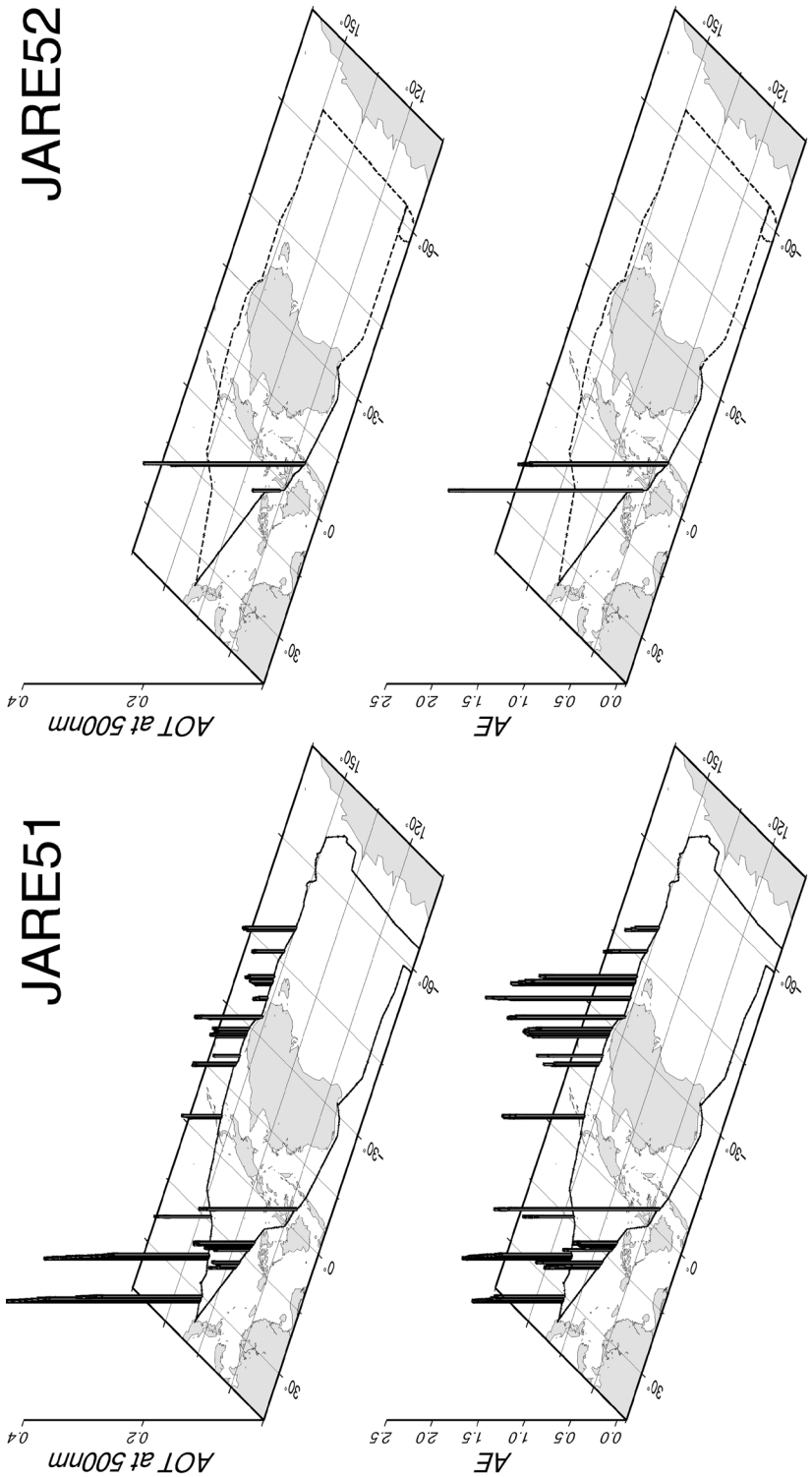

Fig. 5. Spatial distribution of aerosol optical thickness (AOT) at a wavelength of 500 nm and Ångström exponent (AE) along the cruise tracks.

ln F versus m_0 in the logarithm of Equation (1). Figure 4 presents Langley plots at a wavelength of 500 nm. We obtained two data sets in stable cloudless weather over the Tasman Sea. The differences in the calibration constants between these data sets at each wavelength (380, 400, 500, 675, 870, and 1020 nm) were 1.2, 1.7, 1.9, 1.6, 1.3, and 3.1 %, respectively. We adopted calibration constants at each wavelength from the mean of the two data sets. The differences in the minimum and maximum values of AOT at 500 nm were ± 0.003 and ± 0.005, respectively.

Figure 5 shows the distribution of AOT at a wavelength of 500 nm along the ship's tracks. A broken line indicates a track during which the instrument failed because of a breakdown of the electronic circuit. In JARE-51, there were no data from December 4, 2009 to February 26, 2010 in the Antarctic Ocean because of unsuitable sky conditions (cloudy or rainy days). In JARE-52, the instrument failed after the R/V *Shirase* left Fremantle. Consequently, no data were acquired over the Antarctic Ocean during either JARE-51 or JARE-52. However, we did obtain AOT data for other oceans. The number of measurement points was 1237, spread over 16 days of the data set. AOT ranged from 0.01 to 0.34, with particularly high measurements over the western Pacific Ocean on the return from Antarctica and over the seas near Southeast Asia. Deviations in the AOT spectra at 380, 870, and 1020 nm wavelengths were relatively large, particularly for lower AOT values. These large deviations and associated uncertainties can be attributed to the low signal-to-noise ratio of the measurement because the direct solar radiant flux is relatively small in the near-ultraviolet and near-infrared wavelength regions. The AE was calculated from the AOT at 400, 500, and 675 nm. The AE ranged from -0.06 to 2.00, and was particularly high around Southeast Asia and Sydney.

4. Summary

The sun-tracking performance of the shipborne sky radiometer was improved to attain accurate AOTs from direct solar measurements on a pitching and rolling vessel. Improvements were made to the accuracy of sun-pointing measurements, field-of-view expansion, sun-tracking speed, and measurement method. To assess the radiometer's sun-tracking performance and derive AOT and AE over the ocean, radiometric measurements of direct solar and sky brightness distribution were performed onboard the R/V *Shirase* during JARE-51 (2009–2010) and JARE-52 (2010–2011). The temporal variation of signal intensity under clear conditions was smooth, which demonstrated the POM-01 MK3's ability to measure direct sunlight onboard the R/V. The number of data measurement points was 1237, spread over 16 days of the data set. The AOT ranged from 0.01 to 0.34, and values over the western Pacific Ocean in spring and over the Southeast Asia region were higher than over other regions. AE values ranged from -0.06 to 2.00, and were highest over Southeast Asia and off the Australian coast near Sydney. In the future, radiometers incorporating these improvements will contribute to a good understanding of the nature of aerosols over the ocean.

Acknowledgments

This work was undertaken as part of an Antarctic research project named "Study on the material cycle over the Southern Ocean and Antarctic coast: Ship-based measurements" (PI: Masahiko Hayashi), and was supported by members of JARE-51 and JARE-52. The authors especially thank Mr. Yasuo Takeda, Dr. Seizi Koga, Mr. Takuya Masunaga, Mr. Takeshi Kinase, and the crew of the R/V *Shirase* during JARE-51 and JARE-52. The shipboard meteorological data were acquired by the R/V *Shirase* meteorological observation team and were made available via the data acquisition system installed by Prof. Yoshifumi Nogi.

References

Andreae, M.O. (2007): Aerosols before pollution. Science, **315**, 50–51, doi:10.1126/science.1136529.

Aoki, K. and Fujiyoshi, Y. (2003): Sky radiometer measurements of aerosol optical properties over Sapporo, Japan. J. Meteor. Soc. Japan, **81**, 493–513, doi:10.2151/jmsj.81.493.

Holben, B.N., Eck, T.F., Slutsker, I., Tanré, D., Buis, J.P., Setzer, A., Vermote, E., Reagan, J.A., Kaufman, Y.J., Nakajima, T., Lavenu, F., Jankowiak, I. and Smirnov, A. (1998): AERONET—A federated instrument network and data archive for aerosol characterization. Remote Sens. Environ., **66**, 1–16, doi:10.1016/S0034-4257(98)00031-5.

Intergovernmental Panel on Climate Change (2007): Climate Change 2007: The Physical Science Basis. Cambridge, Cambridge University Press, 996 p.

Kaufman, Y.J., Tanré, D., Gordon, H.R., Nakajima, T., Lenoble, J., Frouin, R., Grassl, H., Herman, B.M., King, M.D. and Teillet, P.M. (1997): Passive remote sensing of tropospheric aerosol and atmospheric correction for the aerosol effect. J. Geophys. Res., **102**, 16815–16830, doi:10.1029/97JD01496.

Knobelspiesse, K.D., Pietras, C., Fargion, G.S., Wang, M., Frouin, R., Miller, M.A., Subramaniam, A. and Balch, W.M. (2004): Maritime aerosol optical thickness measured by handheld sun photometers. Remote Sens. Environ., **93**, 87–106, doi:10.1016/j.rse.2004.06.018.

Nakajima, T., Tonna, G., Rao, R., Boi, P., Kaufman, Y. and Holben, B. (1996): Use of sky brightness measurements from ground for remote sensing of particulate polydispersions. Appl. Optics, **35**, 2672–2686, doi:10.1364/AO.35.002672.

Shaw, G.E., Reagan, J.A. and Herman, B.M. (1973): Investigations of atmospheric extinction using direct solar radiation measurements made with a multiple wavelength radiometer. J. Appl. Meteor., **12**, 374–380, doi:10.1175/1520-0450(1973)012 <0374:IOAEUD> 2.0.CO;2.

Shiobara, M., Hayasaka, T., Nakajima, T. and Tanaka, M. (1991): Aerosol monitoring using a scanning spectral radiometer in Sendai, Japan. J. Meteor. Soc. Japan, **69**, 57–70.

Smirnov, A., Holben, B.N., Slutsker, I., Giles, D.M., McClain, C.R., Eck, T.F., Sakerin, S.M., Macke, A., Croot, P., Zibordi, G., Quinn, P.K., Sciare, J., Kinne, S., Harvey, M., Smyth, T.J., Piketh, S., Zielinski, T., Proshutinsky, A., Goes, J.I., Nelson, N.B., Larouche, P., Radionov, V.F., Goloub, P., Krishna Moorthy, K., Matarrese, R., Robertson, E.J. and Jourdin, F. (2009): Maritime aerosol network as a component of aerosol robotic network. J. Geophys. Res., **114**, D06204, doi:10.1029/2008JD011257.

Takamura, T., Nakajima, T. and SKYNET community group (2004): Overview of SKYNET and its activities. Óptica Pura y Aplicada, **37**, 3303–3308.

Yabuki, M., Shiobara, M., Kobayashi, H., Hayashi, M., Hara, K., Osada, K., Kuze, H. and Takeuchi, N. (2003): Optical properties of aerosols in the marine boundary layer during a cruise from Tokyo, Japan to Fremantle, Australia. J. Meteor. Soc. Japan, **81**, 151–162, doi:10.2151/jmsj.81.151.